Sparse Linear Array Synthesis Using Exponential Analysis

Sparse Linear Array Synthesis Using Exponential Analysis

Ramonika Sengupta, Annie Cuyt, David S. Prinsloo, Lukas Nyström and A. Bart Smolders

Abstract—**This paper presents an exponential analysis technique for synthesizing a sparse non-uniform linear array using equidistant samples of the array factor of a dense uniform linear array. The problem statement is explored in a realistic production noise setting (i.e., we model uncertainties/tolerances during production as Gaussian noise), which motivates some slight oversampling. The collected samples are organized in the form of a Hankel matrix. A Cadzow iteration provides an accurate lower-rank approximation of the Hankel matrix. This lower-rank Hankel matrix is then used to obtain an equivalent sparse reduced array that accurately approximates the performance of the original dense array. Numerical experiments demonstrate that the newly developed method is more robust and accurate compared to the methods previously reported.**

Index Terms—**Exponential Analysis, Sparse Array, Array Factor, Gaussian Noise, Hankel Matrix, Cadzow Iteration, Array Synthesis**

I. Introduction

Modern wireless communication systems frequently employ antenna arrays because of their high gain and beamforming capabilities. Recently, unequally spaced sparse arrays that utilize fewer antenna elements are becoming increasingly popular, in terms of reducing the system complexity, cost and power consumption, as well as minimizing the effects of mutual coupling. Several techniques are employed to synthesize sparse linear and planar arrays. Some notable optimization methods include the genetic algorithm [1], where the antenna element positions are optimized in order to achieve a minimum peak sidelobe level, keeping the number of elements and their complex excitations fixed, and simulated annealing [2], where a stochastic method is utilized for synthesizing a planar array from a fully sampled array with half-wavelength element spacing. While these iterative methods have shown promising results for small arrays, they have a tendency to be trapped into local optima resulting in significant computation time when the array is large. Other optimization techniques for array sparsification are presented in [3], [4] and [5]. In [3], a sequence of weighted l_1 convex optimization problems are solved to synthesize a sparse array, and in [4] a multi-objective optimization problem is solved to minimize the number of elements and the peak sidelobe level. In [5], a Bayesian compressive sensing inversion algorithm is proposed to solve a sparseness constrained optimization problem, in order to minimize the number of elements in the array. Other than these iterative methods, non-iterative algorithms using subspace based methods have also been proposed to synthesize sparse linear [6], [7] and planar arrays [8]. Using matrix pencil based algorithms, the methods have successfully reconstructed focused or shaped beam patterns with fewer elements, while also significantly reducing the computation time, when compared to the iterative methods.

In this work, we present a novel exponential analysis approach, for synthesizing a sparse non-uniform linear array. The new approach described in this paper, extends the technique given in [6].

The paper is organized as follows: The problem statement in terms of exponential analysis, along with a discussion of the ill-posed nature of such a problem is described in Section II. In Section III, a new approach for synthesizing a sparse reduced array, using a given uniform dense array, is outlined and compared with the method given in [6]. The examples given in [6] are addressed using the new approach and the results thereof are discussed in Section IV. The conclusions and future work are given in Section V.

II. Problem Statement

Consider the array factor $F(\theta, \phi)$ for a linear array along the x-axis, given by

$$F(\theta, \phi) = \sum_{n=0}^{N-1} I_n \exp\left(jk_0 d_n \sin\theta \cos\phi\right), \qquad (1)$$

where N is the total number of elements in the array, $k_0 = 2\pi/\lambda_0$ is the wavenumber, λ_0 is the wavelength in free space, I_n and d_n are the complex excitation and x-coordinate of the position vector of the n^{th} element respectively, and θ and ϕ are angular coordinates such that $\theta = 0^\circ$ along $\hat{\mathbf{z}}$ and increasing towards $-\hat{\mathbf{z}}$ and $\phi = 0^\circ$ along $\hat{\mathbf{x}}$ and increasing towards $\hat{\mathbf{y}}$, where $\hat{\mathbf{x}}$, $\hat{\mathbf{y}}$ and $\hat{\mathbf{z}}$ are the unit vectors along the x, y and z-axes respectively.

Considering the $\phi = 0^\circ$ plane, we sample $\sin\theta$ of (1) uniformly in $[-1, 1]$ with a sampling interval of $\Delta = 2/(M-1)$, where $M \geq 2N$ is the total number of samples. Two sampling schemes are applicable: an even sampling scheme ($M \geq 2N$ is even) and an odd sampling scheme ($M \geq 2N+1$ is odd). Both sampling schemes give comparable results, hence either can be used for applying

R. Sengupta is with the Department of Electrical Engineering, Eindhoven University of Technology, 5600 MB Eindhoven, The Netherlands (email: r.sengupta@tue.nl).

A. Cuyt is with Computing Science and Mathematics, University of Stirling, Stirling FK9 4LA, Scotland, UK, and also with the Department of Electrical Engineering, Eindhoven University of Technology, 5600 MB Eindhoven, The Netherlands (email: annie.cuyt@stir.ac.uk).

D.S. Prinsloo is with ASTRON, Oude Hoogeveensedjik 4, 7991 PD Dwindloo, The Netherlands, and also with the Department of Electrical Engineering, Eindhoven University of Technology, 5600 MB Eindhoven, The Netherlands (email: prinsloo@astron.nl).

L. Nyström is with SATCUBE, Nellickevägen 22, 41263 Gothenburg, Sweden (email: lukas.nystrom@satcube.com).

A.B. Smolders is with the Department of Electrical Engineering, Eindhoven University of Technology, 5600 MB Eindhoven, The Netherlands (email: A.B.Smolders@tue.nl)

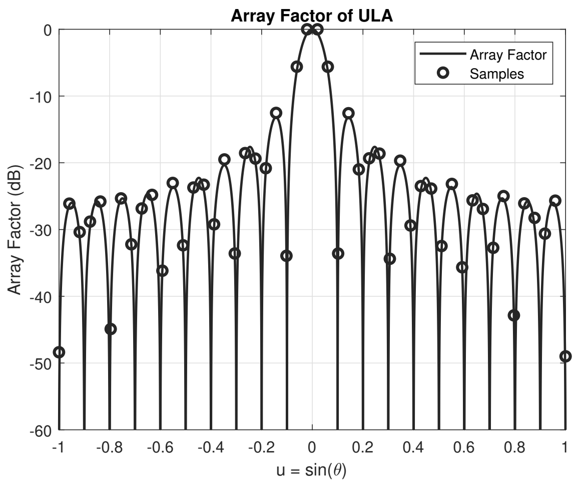

Fig. 1. Array factor of 20 element ULA with uniform excitation

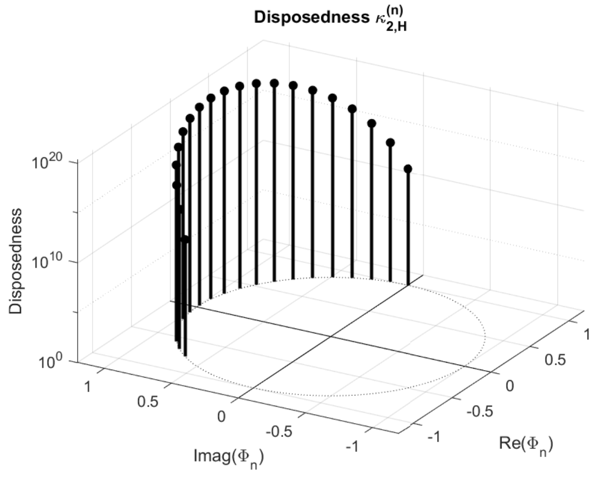

Fig. 2. Disposedness and relative position of Φ_n with $M = 2N$

Prony's method. The array factor in (1) is transformed to a Prony problem [9] as follows:

$$\begin{aligned} F_s &= \sum_{n=0}^{N-1} I_n \exp\left(jk_0 d_n \left(-1 + s\Delta\right)\right), \quad s = 0 \dots M-1 \\ &= \sum_{n=0}^{N-1} \underbrace{I_n \exp\left(-jk_0 d_n\right)}_{r_n} \underbrace{\exp\left(jsk_0 d_n \Delta\right)}_{\Phi_n^s} = \sum_{n=0}^{N-1} r_n \Phi_n^s \end{aligned} \tag{2}$$

where r_n and Φ_n are called the coefficients and the base terms respectively.

Using the array factor samples F_s, one can solve for Φ_n and r_n in order to obtain the original d_n and I_n, or one can solve for an equivalent sparse reduced array

$$\sum_{n=0}^{L-1} \tilde{r}_n \tilde{\Phi}_n^s \approx \sum_{n=0}^{N-1} r_n \Phi_n^s, \quad L < N, \quad s = 0, \dots, M-1. \tag{3}$$

The procedure is explained using an example of a 20 element ULA (uniform linear array) with uniformly excited elements and $\lambda_0/2$ spacing. The array factor is shown in Figure 1.

In order to solve for Φ_n and r_n from the Prony problem (2), $M = 2N$ samples are sufficient. The approximation of the original array by a reduced array with nearby array factor behaviour is possible because the Prony problem is ill-posed [13]. For the purpose of reducing the original linear array, we propose to add realistic production noise ϵ_s to each sample F_s, as explained in Section III, and oversample the array factor, in other words, take $M > 2N + 1$. The disposedness [11] of Φ_n is measured using the Hankel matrix

$$H = \begin{bmatrix} F_0 & F_1 & \dots & F_{\nu-1} \\ F_1 & F_2 & \dots & F_\nu \\ \vdots & \vdots & \ddots & \vdots \\ F_m & F_{m+1} & \dots & F_{M-1} \end{bmatrix}, \tag{4}$$

where $m \geq \nu \geq N$ and $m+\nu = M$. Let the Hankel matrices $H^{(0)}$ and $H^{(1)}$ of size $m \times \nu$ be obtained by respectively removing the last and first rows from H. Here we consider $m = \nu$ (in case M is even) or $m = \nu + 1$ (in case M is odd), such that we obtain (almost) square Hankel matrices in the generalized eigenvalue problem [12]

$$H^{(1)} v_n = \Phi_n H^{(0)} v_n, \tag{5}$$

where the base terms Φ_n are the generalized eigenvalues and the v_n the right eigenvectors.

The disposedness of Φ_n is determined as the upper bound of the relative Euclidean condition number $\kappa_{2,H}^{(n)}(\Phi_n)$ of the generalized eigenvalue problem and is given by [13]

$$\kappa_{2,H}^{(n)}(\Phi_n) \leq \left(|\Phi_n| + 1\right) ||v_n/\sqrt{\alpha_n}||_2^2 \, \frac{||(F_0, \dots, F_{M-1})||_2}{|\Phi_n|} \tag{6}$$

where $\alpha_n = y_n H^{(0)} v_n$ and y_n are the left eigenvectors of the eigenvalue problem (5). In Figure 2 we display the disposedness of the 20 original base terms Φ_n for $m = \nu = N = 20$. Observe that it is indeed quite large ($10^{10} \lesssim \kappa_{2,H}^{(n)} \lesssim 10^{20}$).

Using the new approach discussed in Section III, the disposedness is significantly reduced along with a reduction of the array.

III. New Approach

Let us compute the singular value decomposition (SVD) of H, given by

$$H = U \Sigma W^*, \tag{7}$$

where * denotes the Hermitian transpose, U and W are unitary matrices of size $(m+1) \times (m+1)$ and $\nu \times \nu$ respectively, and Σ is an $(m+1) \times \nu$ diagonal matrix with the singular values $\sigma_1 \geq \dots \geq \sigma_\nu \geq 0$ on its diagonal. Figure 3 shows the log scale plot of the singular values of H for $M = 2N$ samples and hence $m = \nu = N = 20$.

A low rank approximation of H can be obtained by retaining only the largest/principal singular values, and setting the rest to zero. The Hankel matrix H is then approximated by

$$\tilde{H} = U \tilde{\Sigma} W^*, \tag{8}$$

where $\tilde{\Sigma} = \mathrm{diag}\{\sigma_1, \sigma_2, \dots, \sigma_L, 0 \dots 0\}$ with L corresponding to the number of elements in the synthesized array (3).

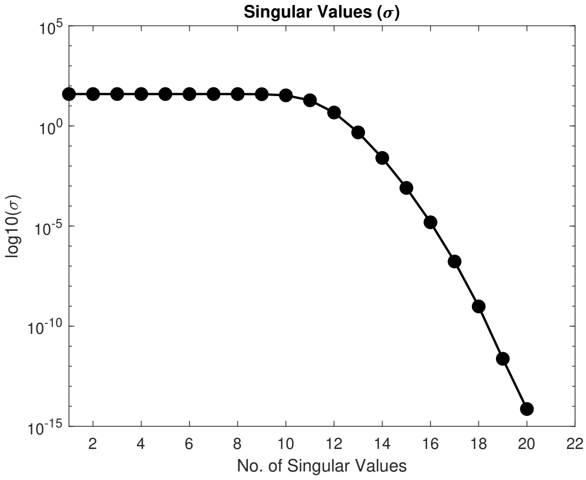

Fig. 3. Log scale plot of singular values σ_i for $M = 2N$ samples

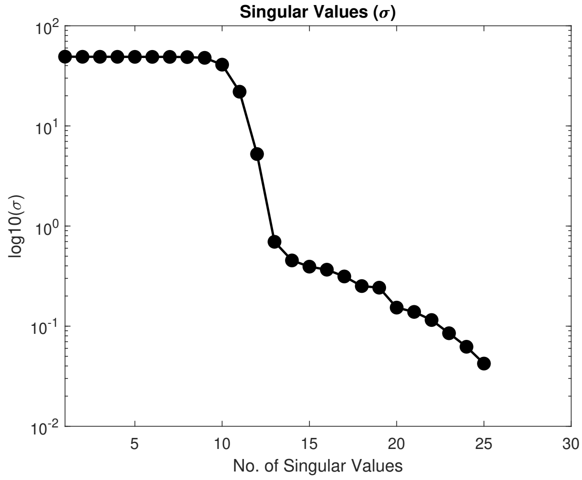

Fig. 4. Log scale plot of noisy singular values σ_i for $M = 2.5N$

The distance between H given in (4) and its low rank approximation $\tilde{H}$, equals [14]

$$\left|\left|H - \tilde{H}\right|\right|_F = \sqrt{\sum_{i=L+1}^{N} \sigma_i^2} \quad , \tag{9}$$

where $||\cdot||_F$ is the Frobenius norm. Determining the appropriate value of L, simply by observing Figure 3, may lead to inaccuracies since it necessitates setting a user-defined tolerance ξ, as in [6], where

$$L = \min \left\{ l : \frac{\sqrt{\sum_{i=l+1}^{\nu} \sigma_i^2}}{\sqrt{\sum_{i=1}^{l} \sigma_i^2}} < \xi \right\}. \tag{10}$$

In order to make L recognizable, we present a new approach that does not require choosing a value for ξ. To this end, we start by adding complex Gaussian noise ϵ_s to the array factor samples F_s,

$$F_s \leftarrow F_s + \epsilon_s, \qquad s = 0 \dots M-1. \tag{11}$$

The level of the noise terms is chosen such that it represents acceptable production noise. For instance, a reasonable assumption regarding the tolerance on the antenna element positions d_n, for an array operating at 1.5 GHz, is somewhere between 25 and 50 micrometers, while for the excitation I_n one has 5- or 6-bit control resolution on the amplitude and phase. Such assumptions amount to around 35 dB SNR for our 20 element ULA. In general, the correct noise level can easily be determined by carrying out a sufficiently high number of simple array factor evaluations.

The singular value plot of the noisy Hankel matrix H with $m = \nu = 25$, is shown in Figure 4. The larger number of samples $M = 2.5N$ also in a way compensates for the poorer quality of the samples due to the added noise. Observe that there is a sharp decrease after σ_{12}, which is also the point of maximum curvature in the singular value plot. From Figure 4 it is more straightforward to determine how many antenna elements contribute to the array factor above the production noise level.

While the addition of noise facilitates the determination of L, the ill-posedness might lead to inconsistent results. Indeed, since an ill-posed problem does not have a unique solution, different noise realizations might result in different arrays. Hence, to improve the reliability of this approach, we obtain a noisy version of H as the average of a few perturbations (11), and we include a Cadzow iteration [15] as an additional step as well.

The Cadzow iteration is initialized by detecting the point of maximum curvature in the singular value plot of the noisy H matrix (which is $L = 12$ in Figure 4) and computing $\tilde{H}$ as in (8) by retaining only the first L singular values. Note here that $\tilde{H}$ is not necessarily Hankel structured anymore. To amend this, one averages in each iteration step over the anti-diagonals in the matrix $\tilde{H}$. The process is repeated by computing the SVD of the "averaged" matrix to obtain an updated L and a new $\tilde{H}$. The iteration stops when $\tilde{H}$ itself is sufficiently close to being Hankel structured. The stopping criterion here can also be formulated in terms of the production noise level:

$$\max_{p+q=k+1} \left| \tilde{H}_{p,q} - \text{mean}_{\ p+q=k+1} \tilde{H}_{p,q} \right| \leq \gamma, \tag{12}$$

where k denotes the antidiagonal (we go through the full matrix $\tilde{H}$) and γ is the threshold value $\gamma = 10^{(-\text{SNR}/20)}$. Figure 5 shows the singular value plot of $\tilde{H}$ after the Cadzow iteration.

Comparing Figures 4 and 5, it is clear that the inclusion of Cadzow inserts a clear gap between the principal and non-principal singular values. Moreover, we obtain $L = 13$ from Figure 5, which indicates that our initial guess of $L = 12$ from Figure 4 was not optimal. Although $L = 12$ would also produce a reasonable synthesis, inclusion of the Cadzow iteration improves the robustness and ensures an optimal L.

With L established, the production noise $\epsilon_s, s = 0, \dots, M-1$ is not required anymore. We proceed with the computation of $\tilde{\Phi}_n$ using noise-free samples F_s in (5). Here, we use $\tilde{H}^{(0)}$ and $\tilde{H}^{(1)}$, obtained from the noise-free $\tilde{H}$ computed from (8) with L delivered by the Cadzow iteration. Note that

$$\tilde{H} = \mathcal{U}\mathcal{S}\mathcal{W}^*, \tag{13}$$

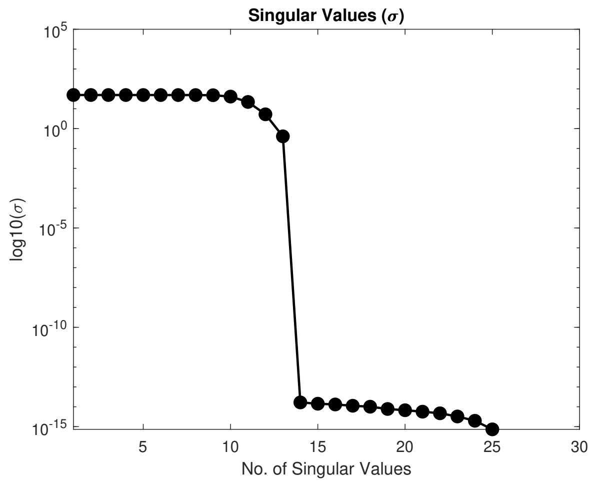

Fig. 5. Log scale plot of singular values post Cadzow iteration

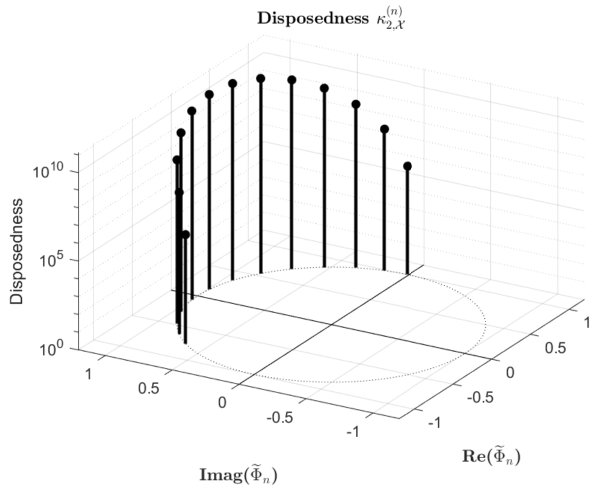

Fig. 6. Disposedness and relative position of $\tilde{\Phi}_n$ with $M = 2.5N$

where $\mathcal{U}$ and $\mathcal{W}$ are of size $(m+1) \times L$ and $\nu \times L$ respectively, obtained by retaining L left and right singular vectors in (8). The matrix $\mathcal{S}$ of size $L \times L$, only has $\sigma_1, \ldots, \sigma_L$ on the diagonal and zero elsewhere.

As earlier, $\mathcal{U}^{(0)}$ and $\mathcal{U}^{(1)}$ are formed by respectively removing the last and first rows from $\mathcal{U}$. Then $\tilde{H}^{(0)}$ and $\tilde{H}^{(1)}$ are given by

$$\tilde{H}^{(0)} = \mathcal{U}^{(0)}\mathcal{S}\mathcal{W}^*, \quad \tilde{H}^{(1)} \approx \mathcal{U}^{(1)}\mathcal{S}\mathcal{W}^*. \tag{14}$$

By introducing $w_n = \mathcal{S}\mathcal{W}^* v_n$, the base terms $\tilde{\Phi}_n$ in (3) are obtained from the eigenvalue problem

$$\mathcal{X} w_n = \tilde{\Phi}_n w_n \tag{15}$$

where $\mathcal{X}$ is the $L \times L$ matrix satisfying $\mathcal{U}^{(0)}\mathcal{X} = \mathcal{U}^{(1)}$. Figure 6 shows the disposedness of $\tilde{\Phi}_n$, given by

$$\kappa_{2,\mathcal{X}}^{(n)}(\tilde{\Phi}_n) \leq \frac{||z_n||_2||w_n||_2}{|{z_n}^* w_n|} \frac{||\mathcal{X}||_2}{|\tilde{\Phi}_n|}, \tag{16}$$

where z_n are the left eigenvectors of the eigenvalue problem (15). Comparing Figures 2 and 6, it is clear that the disposedness is reduced drastically from $10^{10} \lesssim \kappa_{2,H}^{(n)} \lesssim 10^{20}$ to $10^5 \lesssim \kappa_{2,\mathcal{X}}^{(n)} \lesssim 10^{10}$.

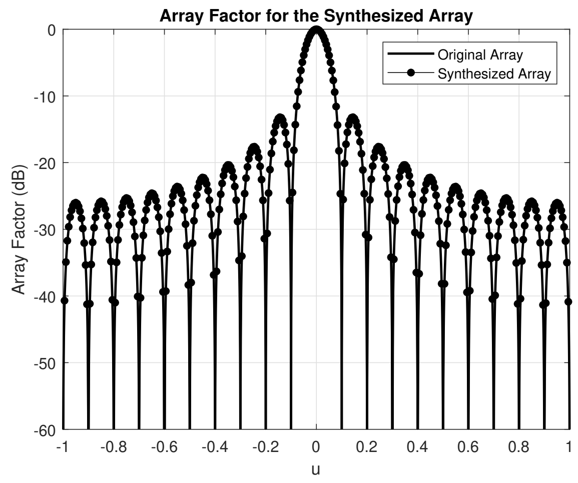

Fig. 7. Array factor of the synthesized array

We calculate $\tilde{r}_n$ by solving the over-determined system of linear equations

$$\begin{bmatrix} 1 & 1 & \ldots & 1 \\ \tilde{\Phi}_0 & \tilde{\Phi}_1 & \ldots & \tilde{\Phi}_{L-1} \\ \vdots & \vdots & \ddots & \vdots \\ \tilde{\Phi}_0^{(M-1)} & \tilde{\Phi}_1^{(M-1)} & \ldots & \tilde{\Phi}_{L-1}^{(M-1)} \end{bmatrix} \begin{bmatrix} \tilde{r}_0 \\ \tilde{r}_1 \\ \vdots \\ \tilde{r}_{L-1} \end{bmatrix} = \begin{bmatrix} F_0 \\ F_1 \\ \vdots \\ F_{M-1} \end{bmatrix}, \tag{17}$$

obtained from (3), using the computed values of $\tilde{\Phi}_n$.

In a final step, we filter out the terms with coefficients of negligible magnitude, meaning less than a few percentages of the term with largest magnitude. This on the one hand ensures that only the main contributing elements remain in the synthesized array, and on the other hand maximizes the sparsity. The final and retained element positions $\tilde{d}_n$ and excitations $\tilde{I}_n$ are recomputed using (15) and (17) with a possibly even smaller L. In case of the 20-term ULA ($N = 20$) synthesized as a 13-term non-uniform array ($L = 13$), the final step did not further decrease L.

Figure 7 shows the array factor of the synthesized array. A good agreement is obtained, with a small error of order 10^{-4}. This approach also automatically reveals a small threshold value $\xi \approx 10^{-5}$ for use in (10). In the end, comparing the Figures 3 and 5, it is very clear that a satisfactory value for L is much easier to obtain from Figure 5 than from Figure 3.

IV. Examples

A. Example 1: Chebyshev Tapering

In this example, we present results for the Chebyshev pattern/array factor given in [6], obtained using the new approach. A Chebyshev tapering [16] is applied to the 20 element uniform array considered in Section III, in order to obtain a side-lobe level SLL $= -30$ dB. Using the same sampling scheme of $M = 2.5N$ and SNR of 35 dB, the reconstructed array factor is shown in Figure 8. With the new approach, a 13 element array is synthesized, resulting in 35% savings in the number of elements. A comparison with the array factor, reconstructed using the method given in [6], with $\xi = 10^{-2}$, is also shown in Figure 8. This alternative method delivers an array with 12 elements. The

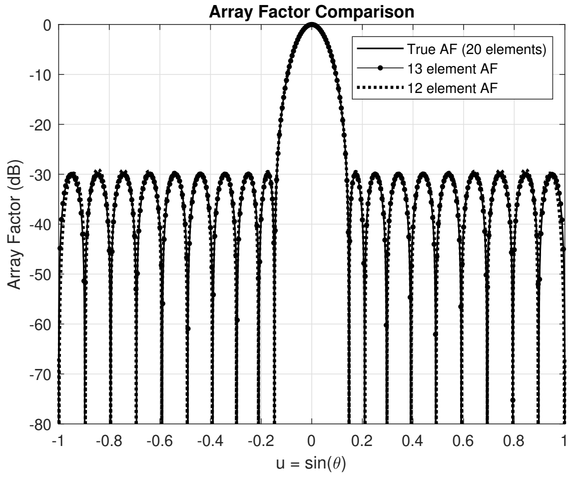

Fig. 8. Chebyshev pattern from [6] reconstructed using the new approach

element positions and excitations are listed in Table I, with the arrays being symmetric about the origin.

With the new approach, the maximum error between the true array factor and the reconstructed array factor is only 5.6×10^{-4}, while ξ equals 1.6×10^{-4}. For the alternative method [6], the error depends on the chosen value of ξ. For $\xi = 10^{-2}$, the error is 7.0×10^{-3}, and for $\xi = 10^{-3}$, a 13 element array is obtained and the error is comparable to the one of the new approach.

Concerning the choice of ξ, any value between 1.6×10^{-4} and 2.2×10^{-3} results in a 13 element array, while for $\xi > 2.2 \times 10^{-3}$, a 12 element array is obtained.

TABLE I
CHEBYSHEV ARRAY COMPARISON WITH [6]

Original Array		Positions and Excitations [6]		Positions and Excitations Using New Approach	
n	I_n	$\tilde{d}_n/\lambda_0$	$\tilde{I}_n$	$\tilde{d}_n/\lambda_0$	$\tilde{I}_n$
0	1	0.425	1	0	1
1	0.970	1.275	0.914	0.819	0.958
2	0.912	2.123	0.760	1.635	0.842
3	0.831	2.967	0.567	2.444	0.673
4	0.731	3.801	0.371	3.238	0.483
5	0.620	4.637	0.268	4.002	0.303
6	0.505			4.712	0.235
7	0.391				
8	0.286				
9	0.326				

B. Example 2: Non-Uniform Array Presented in [17]

For this example, we use the non-uniform array from [17], present results obtained using the new approach and compare them with the results given in [6]. The samples are taken from the desired pattern, shown in Figure 9. With the new approach, we only consider $3N = 51$ samples, rather than 80 samples as in [6]. The SNR considered for this case is 45 dB.

The reconstructed array factor is shown in Figure 9. In [17], the element positions are optimized to generate a pattern using 17 elements. Using the alternative method given in [6], the number of elements is reduced to 13. With the new approach, we obtain a 15 element array. The positions

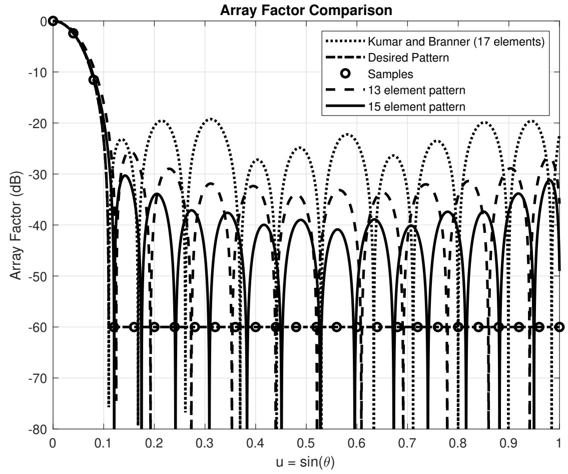

Fig. 9. Reconstructed array factor using the new approach and comparison with [17] and [6]

and excitations are shown in Table II, with the arrays being symmetric about the origin.

It is clear from Figure 9 that the reconstructed pattern from the new approach has a lower SLL compared to both [17] and [6]. Moreover, the pattern is generated using only $3N$ samples from the desired pattern, resulting in savings of about 12% in the number of elements.

TABLE II
ARRAYS SYNTHESIZED BY [17], [6] AND THE NEW APPROACH

Positions [17]		Positions and Excitations [6]		Positions and Excitations Using New Approach	
n	d_n/λ_0	$\tilde{d}_n/\lambda_0$	$\tilde{I}_n$	$\tilde{d}_n/\lambda_0$	$\tilde{I}_n$
0	0	0	1	0	1
1	0.5	0.885	0.959	0.891	0.961
2	1.0	1.770	0.869	1.782	0.876
3	1.5	2.654	0.733	2.672	0.747
4	2.0	3.537	0.569	3.562	0.590
5	2.683	4.418	0.399	4.452	0.425
6	3.464	5.303	0.247	5.341	0.272
7	4.297			6.230	0.146
8	5.163				

C. Example 3: Reconstruction of Pattern from [18]

For this final example, we reconstruct the pattern given in [18] using the new approach. The true pattern for this example, shown in Figure 10, is obtained for a 32 element non-uniform array. Using $2.5N = 80$ samples and an SNR of 35 dB, we obtain a 24 element linear array, identical to the one in [6] for the same example. While the method in [6] requires a pre-defined $\xi = 10^{-3}$ to acquire the principal singular values, the new approach automatically separates the 24 principal singular values from the non-principal ones (see Figure 11).

V. CONCLUSIONS AND FUTURE WORK

A new approach for synthesizing a sparse reduced array, starting from a uniform dense array, is presented. With the new approach, we extend the method described in [6], making it more autonomous and robust. The array factor

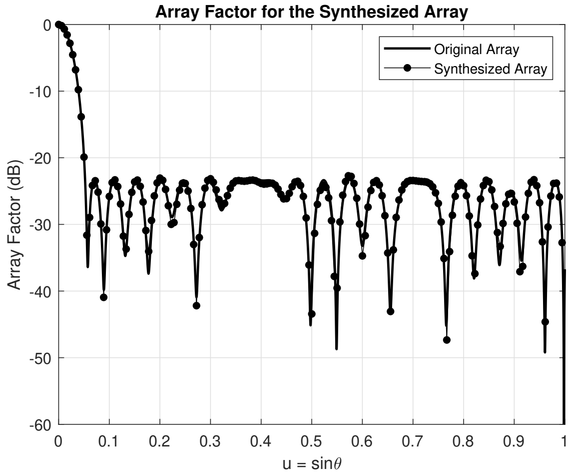

Fig. 10. Pattern from [18] reconstructed using the new approach

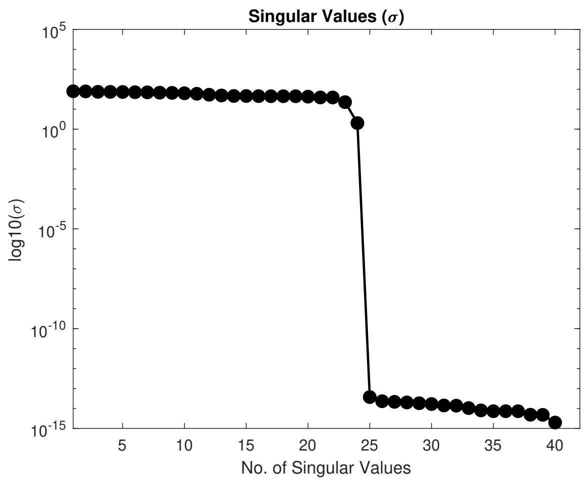

Fig. 11. Log scale plot of singular values post Cadzow iteration for Example 3

expression is rewritten as an exponential analysis problem (2). Due to the inherent ill-posedness of the inverse problem, as discussed in Section II, it is possible to solve for an equivalent sparse reduced array (3). Using a Cadzow iteration, we establish the number of elements in the synthesized array. Compared to [6], the new approach does not depend on user-defined thresholds, while being equally computationally efficient.

Future work to further develop the presented method involves investigating the usage of non-uniform sampling and the support of constraints on the element spacing and antenna dimension. In addition, the implementation of sub-Nyquist sampling schemes is also an area of interest.

Acknowledgment

This project has received funding from the Horizon Europe research and innovation programme under the Marie Skłodowska Curie grant agreement No 101072363.

References

[1] K. Chen, X. Yun, Z. He and C. Han, "Synthesis of Sparse Planar Arrays Using Modified Real Genetic Algorithm," in *IEEE Transactions on Antennas and Propagation*, vol. 55, no. 4, pp. 1067-1073, April 2007, doi: 10.1109/TAP.2007.893375.

[2] A. Trucco, "Thinning and weighting of large planar arrays by simulated annealing," in *IEEE Transactions on Ultrasonics, Ferroelectrics, and Frequency Control*, vol. 46, no. 2, pp. 347-355, March 1999, doi: 10.1109/58.753023.

[3] B. Fuchs, "Synthesis of Sparse Arrays With Focused or Shaped Beampattern via Sequential Convex Optimizations," in *IEEE Transactions on Antennas and Propagation*, vol. 60, no. 7, pp. 3499-3503, July 2012, doi: 10.1109/TAP.2012.2196951.

[4] H. Li, F. He, Y. Chen, and J. Luo, "Multi-objective self-organizing optimization for constrained sparse array synthesis," *Swarm and Evolutionary Computation*, vol. 58, p. 100743, Nov. 2020, doi: https://doi.org/10.1016/j.swevo.2020.100743.

[5] W. Zhang, L. Li and F. Li, "Reducing the Number of Elements in Linear and Planar Antenna Arrays With Sparseness Constrained Optimization," in *IEEE Transactions on Antennas and Propagation*, vol. 59, no. 8, pp. 3106-3111, Aug. 2011, doi: 10.1109/TAP.2011.2158943.

[6] Y. Liu, Z. Nie and Q. H. Liu, "Reducing the Number of Elements in a Linear Antenna Array by the Matrix Pencil Method," in *IEEE Transactions on Antennas and Propagation*, vol. 56, no. 9, pp. 2955-2962, Sept. 2008, doi: 10.1109/TAP.2008.928801.

[7] Y. Liu, Q. H. Liu and Z. Nie, "Reducing the Number of Elements in the Synthesis of Shaped-Beam Patterns by the Forward-Backward Matrix Pencil Method," in *IEEE Transactions on Antennas and Propagation*, vol. 58, no. 2, pp. 604-608, Feb. 2010, doi: 10.1109/TAP.2009.2037709.

[8] K. Yang, Z. Zhao and Y. Liu, "Synthesis of sparse planar arrays with matrix pencil method," *2011 International Conference on Computational Problem-Solving (ICCP)*, Chengdu, China, 2011, pp. 82-85, doi: 10.1109/ICCPS.2011.6089772.

[9] A. Cuyt, Y. Hou, Ferre Knaepkens, and W. Lee, "Sparse Multidimensional Exponential Analysis with an Application to Radar Imaging", *SIAM Journal on Scientific Computing*, vol. 42, no. 3, pp. B675–B695, May 2020, doi: https://doi.org/10.1137/19m1278004.

[10] H. Engl, M. Hanke, and A. Neubauer, *Regularization of inverse problems*. Dordrecht: Kluwer Academic, 1996.

[11] M. Briani, A. Cuyt, F. Knaepkens, and W. Lee, "Vexpa: Validated Exponential Analysis through Regular Sub-Sampling," *Signal processing*, vol. 177, pp. 107722, 2020. DOI:10.1016/j.sigpro.2020.107722.

[12] Y. Hua and T. K. Sarkar, "Matrix pencil method for estimating parameters of exponentially damped/undamped sinusoids in noise," *IEEE Trans. Acoust., Speech, Signal Process.*, vol. 38, no. 5, pp. 814–824, May 1990, doi: https://doi.org/10.1109/29.56027.

[13] B. Beckermann, G. H. Golub, and G. Labahn, "On the numerical condition of a generalized Hankel eigenvalue problem", *Numer. Math.*, vol. 106, no. 1, pp. 41–68, Mar. 2007, doi: https://doi.org/10.1007/s00211-006-0054-x.

[14] I. T. Jolliffe, *Principal component analysis*. New York ; London: Springer, 2011.

[15] J. Gillard, "Cadzow's basic algorithm, alternating projections and singular spectrum analysis," *Statistics and Its Interface*, vol. 3, no. 3, pp. 335–343, 2010, doi: https://doi.org/10.4310/sii.2010.v3.n3.a7.

[16] C. A. Balanis, *Antenna theory : analysis and design*. Hoboken, Nj: Wiley Interscience, 2005.

[17] B. P. Kumar and G. R. Branner, "Design of unequally spaced arrays for performance improvement," in *IEEE Transactions on Antennas and Propagation*, vol. 47, no. 3, pp. 511-523, March 1999, doi: 10.1109/8.768787.

[18] D. G. Kurup, M. Himdi and A. Rydberg, "Synthesis of uniform amplitude unequally spaced antenna arrays using the differential evolution algorithm," in *IEEE Transactions on Antennas and Propagation*, vol. 51, no. 9, pp. 2210-2217, Sept. 2003, doi: 10.1109/TAP.2003.816361.